Eng. & Tech. Journal .Vol. 30, No.19, 2012

Natural Convection Heat Transfer in Enclosure with Uniformly Heated Inner Elliptic Cylinder and Outer square Cylinder

Dr. Akeel Abdullah Mohammed
Petroleum Technology Department, University of Technology/ Baghdad
Email:akeelabdullah@yahoo.com

Received on: 28/12/2011 & Accepted on:4/10/2012

ABSTRACT

Experimental and numerical simulation study for natural convection heat transfer formed by uniformly heated inclined elliptical cylinder concentrically located in an enclosed square cylinder subjected to the ambient have been investigated. Experiments have been carried out for Rayliegh number ranges from 0.9×10^6 to 3.3×10^6. The enclosure angles of inclination are $\phi=0^o$ (horizontal), 45^o (inclined), and 90^o (vertical), and for axis ratio of elliptic cylinder (minor/major=b/c) of 1:2, while the dimensions of outer square cylinder was $0.5\times0.5\times2$ m. A numerical simulation was conducted by using commercial Fluent CFD code to investigate the steady laminar natural convective heat transfer for air between a heated elliptic cylinder and its square enclosure. It covered a range of hydraulic radius ratios (HRR) of 1.97, 2.62, and 3.93 and for orientation angles $\varphi=0^o$ (the major axis is vertical), 30^o, 45^o. Two values of Rayligh number were taken: 0.9×10^6 and 3.3×10^6. The experimental results showed that the heat transfer process improves as Rayliegh number increases and is better in $\phi=0^o$ than other angles of inclination at the same heat input. Theoretical results showed that the HRR, Rayligh number, and angle of orientation have significant effect on the physical behavior of stremlines and isotherms inside the equivalent annular gap.

Keywords: natural convection, square enclosure, elliptic cylinder.

أنتقال الحرارة بالحمل الحر بحيز مغلق بأسطوانة داخلية بيضوية مسخنة تسخين منتظم و أسطوانة خارجية مربعة

الخلاصة

تم دراسة عملية انتقال الحرارة بالحمل الحر المتولدة من قبل أسطوانة بيضوية مائلة تم وضعها بمركز اسطوانة مربعة معرضة إلى المحيط. أجريت التجارب لعدد Ra يمتد من 0.9 $\times10^6$ إلى 3.3×10^6 . زوايا الميل للحيز المغلق هي $\phi = 0^o, 45^o, 90^o$ و نسبة المحور الثانوي إلى الرئيسي للأسطوانة البيضوية 2:3 , في حين كانت أبعاد الأسطوانة الخارجية مستطيلة المقطع $0.5\times0.5\times2$ م . تم أجراء دراسة نظرية بأستخدام برنامج تجاري مخصص للحل العددي لديناميك الهواء للتحري عن عملية أنتقال الحرارة الطبيعي المستقر للهواء بين أسطوانة بيضوية

https://doi.org/10.30684/etj.30.19.12
2412-0758/University of Technology-Iraq, Baghdad, Iraq

مسخنة و أسطوانة مغلقة مربعة . غطت الدراسة العددية نسب نصف القطر الحقيقي 1.97, 2.62, 3.93 وزوايا ميل دورانية $\varphi = 0^o$ (المحور الرئيسي عمودي), 30^o, 45^o. تم أخذ قيمتين لعدد Ra : 0.9×10^6 و 3.3×10^6. بينت النتائج العملية إن عملية انتقال الحرارة تتحسن بزيادة عدد Ra وتكون في حالة $\phi = 0^o$ أفضل من بقية زوايا الميل عند نفس الحرارة الداخلة. بينت الدراسة النظرية إن كل من نصف القطر الحقيقي, عدد Ra , وزاوية الميل الدورانية يمتلكون تأثير كبير على السلوك الفيزيائي لخطوط الجريان و منحنيات درجة الحرارة داخل التجويف الحلقي المكافئ.

INTRODUCTION

As it has been the case for fundamental engineering problems, natural convection in an annular enclosure has been the target of persistent scientific research. The research has been directed to this problem because of its pertinence to many practical engineering applications. These applications include nuclear reactor system, thermal storage and solar heating systems. The function of the outer surface of the enclosure is to reduce the heat transfer from the inner hot surface or to protect the inner body in harsh outdoor environment. The increasing interest in developing compact and highly efficient heat exchanger motivated researchers to study heat transfer from tubes of non-circular cross section. Special attention was focused on tubes of elliptic cross section since they found to create less resistance to the cooling fluid which results in less pumping power in case of forced flow. In case of power failure, natural convection becomes the dominant mode of heat transfer. Moreover, the elliptic tube geometry is flexible enough to approach a circular tube when the axis ratio approaches unity and approaches flat plate when the axis ratio becomes very small.

The problem of natural convection in an annulus between two concentric and eccentric cylinders with different geometries and for both cases open ends and enclosure was considered experimentally and theoretically by many researchers**.** Vafai et al [1] presented a combined experimental and numerical investigation of buoyancy driven flow and heat transfer in a narrow annular gap between co-axial, horizontal cylinders. Results of the conjugate study including the local temperature distribution, heat transfer coefficients, and the flow field showing the interactions between the ambient and cavity flow fields agree with experimental results. Maged and Negm [2] studied theoretically the conjugate natural convection heat transfer in an open-ended vertical concentric annulus with isothermal outer tube and adiabatic inner tube. Results showed that the wall to fluid thermal conductivity ratio has prominent effects on the steady heat transfer parameters. Shu et al [3] studied theoretically the natural convection in a horizontal eccentric annulus between a square outer cylinder and a circular inner cylinder for $Ra=3\times10^6$. It was found that the global circulation, flow separation and the top space between the square outer cylinder and the circular inner cylinder have significant effects on the plume inclination. Maged and Esmail [4] explored effect of the annulus geometrical parameters on the induced flow rate and the heat transfer under the conjugate thermal boundary conditions with one cylinder heated isothermally while the other cylinder was kept at the inlet fluid temperature. The results showed that the geometry parameters (the fluid annulus radius ratio and the eccentricity) have considerable effects on the heat transfer process. Teertstra et al [5] developed an analytical model for natural convection in the two dimensional region formed by an

isothermal, heated horizontal cylinder concentrically located in a larger, cooled horizontal cylinder. Agreement between the model and existing numerical and experimental data from the literature was quite good with an average difference of approximately 6-9% for all cases. Laminar natural convection heat transfer between two horizontal concentric cylinders with two fins attached to inner cylinder was numerically by Alshahrani and Zeitoun [6] using finite element technique. They concluded that the thermal resistance decrease as fin length increases i.e. as an annular gap thickness increases. Eid [7] studied experimentally and numerically the natural convection heat transfer in elliptic annuli with different aspect ratios. The results show that the rotation of the elliptic annuli with small aspect ratio by a right angle whenever the taken specimens are horizontal or inclined improves the free convection heat transfer characteristics. Djezzar et al [8] expressed the Bossiness equations of the laminar thermal and natural convection in the case of permanent and bidimensional flow, in an annular space between two confocal elliptic cylinders. A new calculation code using the finite volumes with the primitive junction (velocity-pressure formulation) and the elliptic coordinates system was proposed. Simulation of natural convection in eccentric annuli between a square outer cylinder and a circular inner cylinder was submitted by Ding et al [9]. They concluded that global circulation occurs when the eccentric annulus is not symmetric about the vertical centerline of the inner circular cylinder. Calcagni et al [10] investigated experimentally and numerically the free convective heat transfer in a square enclosure characterized by a discrete heater located on the lower wall and cooled from the lateral walls. The results showed that an increase of the heat source dimension produces a raise in heat transfer particularly for high Ra. Ahmed Mezrhab et al [11] studied numerically the effect of a single and multiple partitions on heat transfer phenomena in an inclined square cavity. Results showed that, in vertical cavities, the average Nusselt number decreases with decreasing of gap widths and reaches to maximum value at gap width about 0.5 at inclined position. Yasin et al [12] used four different temperature boundary conditions for the square body in a porous triangular enclosure to study natural convection as heated, cooled, neutral and adiabatic. They observed that fluid flow and temperature fields strongly depend on thermal conditions of the body. Sakr et al [13] submitted experimental and numerical studies for natural convection in two dimensional region formed by constant heat flux horizontal elliptic tube concentrically located in a larger, isothermally cooled horizontal cylinder. The results showed that the average Nusselt number increases as the orientation angle of the elliptic cylinder increases from 0^o (the major axis is horizontal) to 90^o (the major axis is vertical). A numerical simulation was conducted by Xu Xu et al [14] to investigate the steady laminar natural convection heat transfer for air within the horizontal annulus between a heated triangular cylinder and its circular cylindrical enclosure. They found that, at constant radius ratio, inclination angles of the inner triangular cylinder have negligible effects on the average Nusselt number. Yasin et al [15] studied numerically the phenomena of natural convection in an inclined square enclosure heated via corner heater. It was observed that heat transfer is maximum or minimum depending on the inclination angle and depending on the length of the corner heaters. Mahfouz et al [16] studied theoretically transient and steady natural convection heat transfer in an elliptical annulus placed at different orientations. The results for local and average Nusselt

numbers were obtained and discussed together with the details of both flow and thermal fields. Salam and Ahmed [17] performed numerical study of two dimensional steady natural convection for a uniform heat source applied on the inner circular cylinder in a square enclosure in which all boundaries were assumed to be isothermal. It was found that the total average Nusselt number behaves nonlinearly as a function of locations. They submitted another analysis of steady natural convection of water in inclined square enclosure with internal heat generation [18]. Results showed that as the inclination angle increases, the hydrodynamic boundary layer at the hot and cold side walls decreases. Xu Xu et al [19] carried out another numerical investigation of laminar natural convection heat transfer around horizontal cylinder to its concentric triangular enclosure. The effects of the Rayliegh number and aspect ratio were examined. Zi-Tao Yu et al [20] studied numerically unsteady natural convection heat transfer in a horizontal annular region bounded by a heated inner circular cylinder and coxial outer triangular cylinder. The flow development and the time-averaged Nusselt number over the inner circular wall were predicted. Hang Wang et al [21] examined the laminar flow pattern and thermal stratification by natural convection in a circular enclosure with a rectangle cylinder. Results showed that the vortex occurring on the top of the rectangle cylinder had considerable effects on the average Nusselt number.

However, the lack of detailed information and configuration on the heat transfer in a symmetric and asymmetric annulus formed between uniformly heated elliptic cylinder placed centrally in square enclosure was first motivation for this study. The primary objective of present study is to extend experimentally the knowledge of the temperature distributions, local heat transfer distributions, and overall heat transfer coefficient for inclined enclosure with uniformly heated inner elliptic cylinder at Ra ranges from 0.9×10^6 to 3.3×10^6. Also, the experimental results are extended through the numerical simulation of the present problem to investigate the effect of Rayliegh number, orientation angle, and hydraulic radius ratio HRR of the equivalent annular gap on the heat transfer process.

EXPERIMENTAL SETUP

A schematic representation of the test section assembly used in the present experimental study is shown in Figure (1) It consists of the test section, an electric heater, a voltmeter, an ammeter, an altering variance unit, certain number of calibrated K-type thermocouples and a digital thermometer. The test section mainly consists of two concentric elliptical and square cylinders to form an enclosure region containing air at the atmospheric pressure. The outer square cylinder has dimensions 50×50×200 cm and is made of aluminum except the topside which is made of plexiglass. The length of enclosure is large enough to justify neglecting the end effects. The inner elliptical cylinder was made also of aluminum with a major and minor diameters of 40 and 20 cm (Dh=25.3 cm) and length of 160 cm as shown in Figure (2) The inner elliptical cylinder was heated electrically using an electrical heater which consists of a nickel-chrome wire ®, wound as a coil spirals around solid Teflon elliptical cylinder with 20 cm major diameter and 10 cm minor diameter, and is covered by a 2 mm thickness asbestos layer. This Teflon elliptic cylinder is fitted inside the inner elliptic cylinder, and the space between them is filled with a fine grade sand to avoid heat convection in it and to smooth out any

irregularities in the heat flux. Adjustable screws are used to hold and support the outer square cylinder with the inner elliptic cylinder centrally. Fourteen k-type thermocouples were used to measure the local surface temperatures of the top outer surface of the inner elliptic cylinder along the axial direction. In addition to nine thermocouples at three sections along elliptic cylinder were positioned and arranged at equal angles (four thermocouples at each section). Four additional thermocouples were positioned at the inlet and outlet annular gap (two for each position) to measure the average of air temperatures. On the other hand, ten thermocouples were used to measure the surface temperature of the square cylinder. All thermocouples were used with leads, the thermocouple with lead and without lead were calibrated against the melting point of ice made from distilled water and the boiling points of several pure chemical substances. The readings of the thermocouples are taken by means of a digital thermometer with an accuracy of ±0.1 ^{o}C. The steady-state condition is achieved after 3 to 4 hours approximately. The input electric power to the inner cylinder is controlled by means of a voltage regulator.

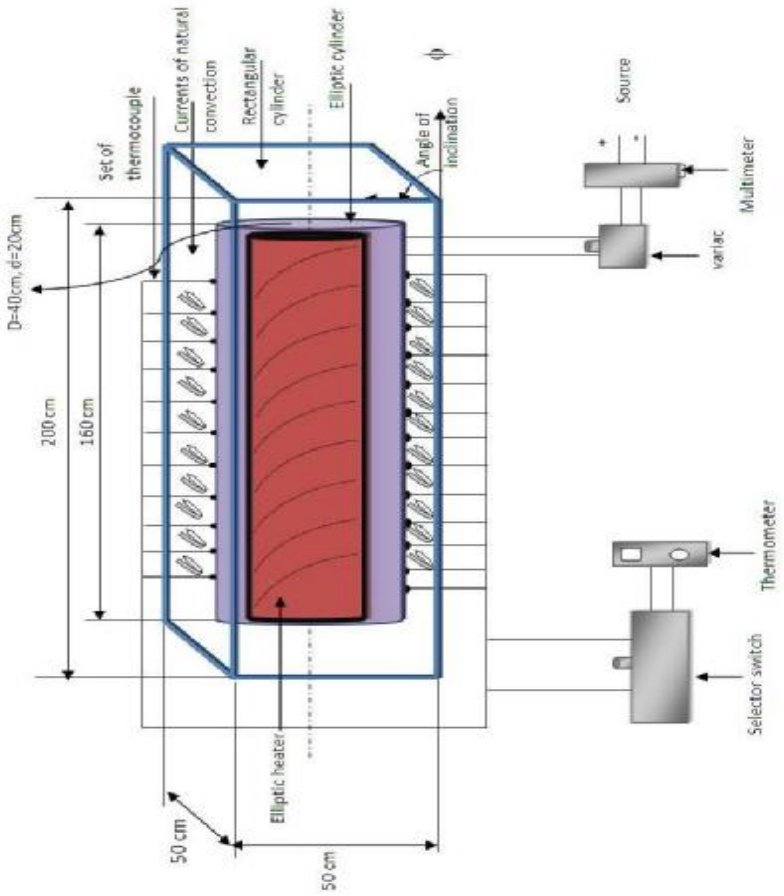

FigURE.(1): Schematic of the experimental rig.

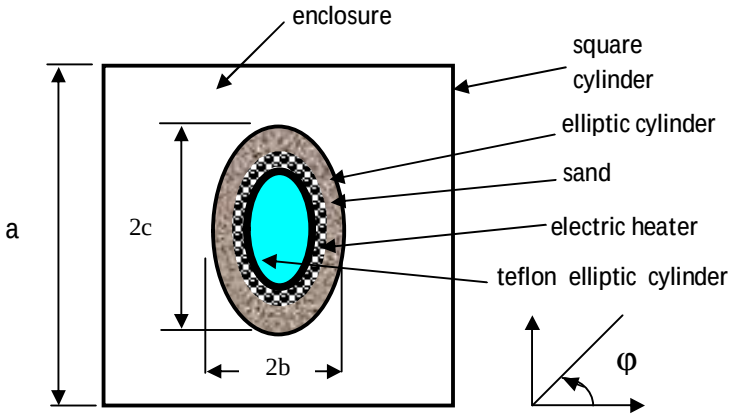

Figure (2): Cross-section of experimental rig.

Data Reduction

The heat transfer by natural convection can be evaluated as follows [7]:

$Q_{conv.}=Q_{total}-Q_{rad.}-Q_{cond}$ ….(1)

where

$Q_{total}=V\times I$ ….(2)

The heat transfer by radiation from inner surface to outer one and to air in the annulus can be found as follows [7];

$$Q_{rad.}=\left[\left(\frac{sP_iL(T_i^4-T_o^4)}{1/e_i+((1-e_o)/e_o)P_i/P_o}\right)+\left(sP_iLe_i(T_i^4-T_o^4)\right)\right] \quad \text{....(3)}$$

where,

T_i and T_o are the average temperature of the inner and outer cylinder, respectively; and P_i & P_o are the perimeters of the outer surface of inner elliptic cylinder and outer square cylinder, respectively. The perimeter of elliptic cylinder is given as:

$$P_i=2\pi\sqrt{\frac{b^2+c^2}{2}} \quad \text{....(4)}$$

but, $\varepsilon_i=\varepsilon_o=\varepsilon$ = emissivity of polished aluminum surface=0.09

Hence, Eq.(3) becomes:

$$Q_{rad.}=\left(seLP_i(T_i^4-T_o^4)\right)\left[\frac{2+(1-e)(P_i/P_o)}{1+(1-e)(P_i/P_o)}\right] \quad \text{....(5)}$$

The heat transfer by conduction Q_{cond} from the two ends of the elliptic cylinder can be found as follows:

$$Q_{cond.} = \frac{T_i - T_e}{2\left(\frac{\Delta x}{\kappa_t . A_t}\right)} \qquad \ldots.(6)$$

where, T_i and T_o are the average temperature of inner and outer surface of Teflon piece.

The local convective heat transfer coefficient, average Nusselt number and Rayleigh number can be found as follows [7, 13]:

$$h_x=Q_{conv.}/P_iL(T_{ix}-T_c) \qquad \ldots.(7)$$

where,

T_{ix} and T_c are the local temperature of inner heated elliptic cylinder and outer cold square cylinder, respectively.

$$h_m=\frac{1}{L}\int_0^L h_x dx \qquad \ldots..(8)$$

$$Nu_m = \frac{h_m D_h}{\kappa_a} \qquad \ldots..(9)$$

where,

$$Gr= gbqr_o D_h^3 / n^2 k_a \qquad \ldots..(10)$$

where Dh is the hydraulic diameter of the elliptic cylinder.

$$Ra=Gr.Pr \qquad ....(11)$$

$$D_h = 4A/P \qquad \ldots..(12)$$

$$D_h)_{eq.} = a - \frac{2\sqrt{2}bc}{\sqrt{b^2 + c^2}} \qquad \ldots..(13)$$

The air properties in the above equations are evaluated at the mean temperature [7]:

$$T_m = \frac{T_w + T_c}{2} \qquad \ldots.(14)$$

where T_w is the average heated wall temperature.

NUMERICAL ANALYSIS

The numerical model consists in a two-dimensional steady isothermal square cavity (cold wall T_c=300 K) with uniformly heated elliptic inner cylinder (hot wall). The length of enclosure is large enough to justify neglecting the end effects;

therefore the air enclosure may be considered as a two-dimensional square cavity. The numerical study has been carried out with the commercial finite volumes code Ansys (Fluent 13.0) designed for the solution of incompressible fluid dynamic problems using with a two-dimensional model and Boussinesq approximation for air (Pr=0.707). The computational scheme that is used by Fluent Inc. [22] is based on the finite volume discretization method, which was described in sufficient detail by Patankar [23] and Versteegh and Malalasekera [24]. FLUENT uses SIMPLE algorithm [25] for pressure–velocity coupling. Choudhury [26] has reported fluid flow and heat transfer calculation using FLUENT for two benchmark problems. One of them was laminar natural convection. The investigation deals with the cases of Rayleigh numbers 0.9×10^6 (q=165 W/m^2) and 3.3×10^6 (q=1080 W/m^2) i.e, the same values indicated in the experimental study. The analysis uses a mesh structure with square grid size 50×50. The computational domain resulted from the subtraction of the elliptical cylinder section from the square cylinder section. A total number of about 1869, 2124, and 2343 nodes are employed for the entire flow domain of hydraulic radius ratio HRR 1.97, 2.62, and 3.93, respectively, to attain grid independent solutions. The governing equations of continuity, momentum, and energy can be written as follows [12, 17, 18, 21, 27]:

$$\frac{\partial u}{\partial x}+\frac{\partial v}{\partial y}=0 \qquad \ldots.(15)$$

$$u\frac{\partial u}{\partial x}+v\frac{\partial u}{\partial y}=g\beta(T-T_w)\sin\varphi-\frac{1}{\rho}\frac{\partial p}{\partial x}+\vartheta\left(\frac{\partial^2 u}{\partial x^2}+\frac{\partial^2 u}{\partial y^2}\right) \qquad \ldots..(16)$$

$$u\frac{\partial v}{\partial x}+v\frac{\partial v}{\partial y}=g\beta(T-T_w)\cos\varphi-\frac{1}{\rho}\frac{\partial p}{\partial y}+\vartheta\left(\frac{\partial^2 v}{\partial x^2}+\frac{\partial^2 v}{\partial y^2}\right) \qquad \ldots\ldots(17)$$

$$\rho C_p\left(u\frac{\partial T}{\partial x}+v\frac{\partial T}{\partial y}\right)=\kappa\left(\frac{\partial^2 T}{\partial x^2}+\frac{\partial^2 T}{\partial y^2}\right) \qquad \ldots.(18)$$

Each computational iteration is solved implicitly. The convergence of the computational solution is determined on scaled residuals for the continuity, energy equations and for many of predicted variables. The settings for the scaled residuals for solution convergence are set to 10^{-3} for nearly all computed residuals. The only exception is the residuals for the energy equation which is set 10^{-6}. The solution is considered to be converged when all of the scaled residuals are less than or equal to these default settings.

RESULTS AND DISCUSSION

A. Experimental Part

The effect of inclination angle on the local temperature distribution along the axis of elliptic inner tube for Ra=0.9×10^6 is shown in **Fig.(3)**. As can be seen from this figure that the values of temperature decrease as angle of inclination deviates from vertical ϕ=90° to horizontal position ϕ=0°. The temperature gradient inside the enclosure causes an upward velocity of the light air near the inner hot surface. While, the heavy air near the cold outer surface moves downward. The opposite movements of light and heavy air create a complete circulation pattern. The

deviation of enclosure towards the horizontal position causes an increase in the circulation of the air around the elliptic inner tube which increases the upward buoyancy-driven plume (i.e., increasing of the currents of natural convection) . As a result, increasing of thermal boundary layer will be accelerated and leads to reduction of temperature values. The temperature value along the elliptical tube of enclosure increases as Rayliegh number increases for the same angle of inclination ϕ=90^o as shown in Figure (4) because of faster increasing of the thermal boundary layer as heat flux increases (i.e., increasing of buoyancy effect as Ra increases). It is noticed also from Figure (3) and Figure(4) that the temperature varies linearly with the longitudinal axis of elliptic inner tube. Figures(5 and 6) illustrate the effect of Rayliegh number on the local Nusselt number along elliptic inner cylinder at $\phi = 0^o$ (horizontal position) and $\phi = 90^o$ (vertical position), respectively. At any angle of inclination, the increasing of Rayleigh number leads to enhancement the heat transfer process within the annulus significantly. The onset of the thermal convection currents brings about the formation of thinner boundary layer along the inner cylinder. The Effect of angle of inclination on the local Nusselt number along elliptic inner cylinder for Ra=0.9×10^6 and 3.3×10^6 are shown in Figure(7) and Figure(8), respectively. It is obvious from these two figures that the values of the local Nusselt number increase as angle of inclination deviates from vertical to horizontal position. As explained before, the free convection for horizontal position creates a longitudinal vortex along the elliptic heated cylinder which its intensity reduces as the angle of inclination moves from horizontal to vertical position leads to reducing of heat transfer coefficient. The cellular motion behaves so as to reduce the temperature difference between the heated elliptic cylinder surface and the hot air flow upword towards outer square cylinder in the enclosure gap, leads to increase the growth of the hydrodynamic and thermal boundary layers along the elliptic cylinder and causes an improvement in the heat transfer coefficient as Ra number increases and as angle of inclination moves from vertical to horizontal position.

The values of the mean Nusselt number are plotted in Figure(9) in the form of log(Nu_m) against log(Ra) for the range of Ra from 0.9×10^6 to 3.3×10^6 and for three angles of inclination ϕ=0^o, 45^o, and 90^o. All points as can be seen are represented by linearization of the following equations:

$$Nu_m = 3.623\ Ra^{(0.053)} \qquad \phi = 0^o \qquad \text{....(19)}$$

$$Nu_m = 3.221\ Ra^{(0.042)} \qquad \phi = 45^o \qquad \text{....(20)}$$

$$Nu_m = 2.831\ Ra^{(0.021)} \qquad \phi = 90^o \qquad \text{....(21)}$$

B. Theoretical Part

Stream Lines

A composite diagram of the streamlines for all cases at $j = 0^o$ is displaced in Figure(10) in which the subfigures are arranged going from left to right with ascending Rayliegh number and going down with descending hydraulic radius ratio HRR. As shown in Figure(10), the annular domain can be roughly divided into three regions, i.e., two upper regions and the lower region below the bottom of the elliptic cylinder. In general, the air heated by the elliptic wall rises and is then cooled down and falls along the outer square enclosure, thus leading to a main

recirculating cell in each upper region. It is also clearly shown that streamlines are distorted below the half of enclosure and the distortion becomes more remarkable with decreasing HRR and increasing Rayliegh number. At HRR=1.97 the streamlines become more concentrated next to the walls, and the cell patterns for Ra=0.9×10^6 is totally different from this for Ra=3.3×10^6 because the stronger stretching effect yields more stratified streamlines. At HRR=1.97 and Ra=3.3×10^6, the streamlines in the middle regions are nearly flat. A composite diagram of the streamlines for all cases at $j = 30^o$ and 45^o are displaced in Figsure(11&12), respectively, in which the subfigures are arranged going from left to right with ascending Rayliegh number and going down with descending hydraulic radius ratio HRR. The most evident feature in these subfigures is that the appearance of strongly asymmetric flow patterns when the equivalent annular enclosure is rotated. This is due to that the symmetric plane of the domain of interest is no longer along the gravitational direction after being rotated. As a matter of fact, the main recirculating cell in the right upper region separates into at least two vortex cores close to each other especially at $j = 30^o$ as shown in Figure(11) and tend to diverge at $j = 45^o$ and Ra=3.3×10^6 as shown in Figure(12-a). As the radius ratio is lowered, the influence of the inclination angle becomes more remarkable. Multicell flow patterns appear when $j = 30^o$ and HRR=1.97 for both taken values of Ra as shown in Figure(11-c). It is obvious also that as φ increases and as HRR decreases the boundary layer separation from lower part of elliptic cylinder becomes more pronounced. The effect of Rayliegh number is small for both $j = 30^o \& 45^o$ and HRR=2.62 & 1.97 as shown in Figure(11-b & c) & Figure(12-b & c), respectively; because the dominant HRR on the heat transfer process more than the relatively small difference between two values of Ra.

TEMPERATURE CONTOURS

The isotherms for various HRR and φ are displaced in Figures(13, 14, and 15) as a composite diagram with the same arrangement as Figures(10, 11, and 12), respectively. In many cases, strong thermal stratification still exists. It is observed from Figure(13) that the isotherms contours is relatively symmetric about the major axis of the elliptic cylinder for inclination angle $j = 0^o$. A thermal plume above the elliptic cylinder is observed for all inclination angles. It is noted that as the orientation angle decreases the temperature level decreases, indicating that more cooling for the elliptic cylinder surface, i.e., higher heat transfer rate with decreasing of the orientation angle. It is observed also that the increase in the major axis length (i.e., decrease in HRR) of the thermal ellipse increases the resistance against the air plume for both taken values of Rayliegh numbers. As a consequence, an intense reduction in the free convective heat transfer was noted for lower HRR. This reduction in the heat transfer inside the equivalent hydraulic annular gap is reduced as the inclination angle increases. The other physical behavior for the increase natural heat transfer in high HRR is may be attributed also to the longer path of the air fluid layer with higher velocity at higher HRR. The isotherms are nearly horizontal at $j = 45^o$, HRR=2.62 & 1.97 and at any Ra as shown in Figure(15-a & b), indicating the conduction heat transfer is the basic

mode. When HRR=3.93 as shown in Figure(15-a), the temperature become to confuse in shape and highly diverge from the linear form indicating that the convection heat transfer is the basic mode. This feature is noted also in Figure(14-c) at HRR=1.97 & $j = 30^o$.

CODE VALIDATION

Due to the lack of published experimental and theoretical data for the geometry concerned in the present study, bench marching theoretical results for the uniformly heated circular cylinder immersed in the square enclosure filled with air by Salam and Ahmed [17] and for the isothermal circular enclosure with inner rectangle cylinder by Hang Wang et al [21]. As shown in **Fig.(16)** & **Fig.(17)**, good agreement was achieved between these works and the present work for both the stream lines and temperature contours. These validation make a good confidence in the present simulation model.

CONCLUSIONS

1. The heat transfer coefficient increases as Rayliegh number Ra increases.
2. The deviation of enclosure from vertical towards the horizontal position causes an increase in the circulation of the air around the elliptic inner cylinder which increases the free convection heat transfer.
3. An empirical equations for average Nusselt number as a function of Rayliegh number are correlated for each angle of inclination ϕ.
4. The appearance of strongly asymmetric flow patterns when the equivalent annular enclosure is rotated.
5. As the orientation angle φ increases and hydraulic radius ratio HRR decreases the boundary layer separation from lower part of elliptic cylinder becomes more pronounced.
6. A thermal plume above the elliptic cylinder is observed for all orientation angles.
7. The reduction in the heat transfer inside the equivalent hydraulic annular gap resulted from increasing of the major axis length of heated elliptic cylinder (lower HRR) is reduced as the orientation angle increases.
8. When the internal Rayliegh number increases above the critical value (10^6), the streamlines and temperature contours become to confuse in shape and seem to be unsymmetrical about the vertical axes that divides the enclosure in two equal parts in the case of vertical position. So, more the researchers take the value of Ra less than or equals 10^6 in the case of laminar natural convection.

Nomenclature

symbol	meaning	symbol	meaning
A_t	area of Teflon piece (m^2)	Q	heat transfer rate (W)
b	minor axis length (m)	q	heat flux (W/m^2)
c	major axis length (m)	Ra	Rayleigh number=Gr.Pr
D_h	hydraulic diameter (m)	T	temperature (^oC)
g	gravity acceleration (m/s^2)	ΔT	temperature difference (^oC)

Gr	Grashof number= $\frac{gbqr_o D_h^3}{n^2 k_a}$	t	inner cylinder thickness (m)
h	heat transfer coefficient ($W/m^2.k$)	u	velocity in x-direction (m/s)
L	length of inner elliptic cylinder (m	V	voltage (volt)
I	current (Amp)	v	velocity in y-direction (m/s)
Nu	Nusselt number= hD_h / κ_a	x	axial position (m)
P	perimeter (m)	Δx	thickness of Teflon piece (m)
Pr	Prandtl number= $\mu c_p / \kappa_a$		

Greek symbols

symbol	meaning
α	thermal diffusivity (m^2/s)
β	volume coefficient of expansion (k^{-1})
ε_i	emissivity of polished aluminum surface=0.09
ϕ	angle of inclination (degree)
φ	angle of orientation (degree)
υ	kinematical viscosity (m^2/s)
μ	dynamic viscosity (Pa.s)
ρ	density (kg/m^3)
σ	Stefan-Boltzman constant =5.6687×10^{-8} ($W/m^2.k^4$)
κ_t	thermal conductivity of Teflon piece ($W/m^2.^oC$)
κ_a	thermal conductivity of air ($W/m^2.^oC$)

Subscripts

symbol	meaning	symbol	meaning
cond.	conduction	m	mean
conv.	Convection	rad.	radiation
eq.	equivalent	s	solid
i	inner	w	wall
o	outer		

REFERENCES

[1]. Vafai K., Desal C. P., Lyer S. V., and Dyker M. P., "Buoyancy induced convection in a narrow open-ended annulus", Transactions of ASME, J. Heat Transfer, Vol. 119, pp. 483-494, August 1997.

[2]. El-sharawi M. A. I. and Negm A. A. A., "Conjugate natural convection heat transfer in an open ended vertical concentric annulus", Numerical Heat Transfer, Part A, 36, pp. 639-655, 1999.

[3]. Shu C., Xue H., and Zhu Y. D., " Numerical study of natural convection in an eccentric annulus between a square outer cylinder and a circular inner cylinder using DQ method", Int. J. Heat and Mass Transfer, Vol. 44, pp. 3321-3333, 2001.

[4]. El Shaarawi M. A. I. and Esmail M. M. A., " Numerical Investigation of conjugate Natural convection heat transfer in vertical eccentric annuli", 4th Int. Conference on Computational Heat and Mass Transfer, 2004.

[5]. Teertstra P., Yovanvich M. M. and Culham J. R., "Analytical modeling of natural convection in horizontal annuli", American Institute of Aeronautics and Astronautics (AIAA)-0959, pp. 1-10, 2005.

[6]. Alshahrani D. and Zeitoun O., " Natural convection in air-filled horizontal cylindrical annuli", Alexanderia Eng. J., Vol. 44, No. 6, pp. 813-823, 2005.

[7]. Eid E. I., "Natural convection heat transfer in elliptic annuli with different aspect ratios", Alexandria Engineering Journal, Vol. 44, No. 2, pp. 203-215, March 2005.

[8]. Djezzar M., Chaker A., and Daguenet M., "Numerical study of Bidimensional steady natural convection in a space annulus between elliptic confocal ducts influence of the internal eccentricity", Rev. Energ. Ren., Vol. 8, pp. 63-72, 2005.

[9]. Ding H. , Shu C. , and Yeo K. S., "Simulation of natural convection in eccentric annuli between a square outer cylinder and a circular inner cylinder using local MQ-DQ method"; Numerical Heat Transfer, Part A, 47: 291–313, 2005.

[10]. Calcagni B., Marsili F., Paroncini M., "Natural convective heat transfer in square enclosures heated from below", Applied Thermal Engineering 25, pp. 2522–2531, 2005.

[11]. Ahmed M., Mohammed J., Cherifa A., Mohamed B., and Pierre L., "Lattice-Boltzmann modeling of natural convection in an inclined square enclosure with partitions attached to its cold wall"; International Journal of Heat and Fluid Flow 27 (2006) 456–465.

[12] Yasin V., Hakan F. O.,Tuncay Y.,"Two-dimensional natural convection in a porous triangular enclosure with a square body"; International Communications in Heat and Mass Transfer 34 (2007) 238–247.

[13]. Sakr R. Y., Berbish N. S., Abd-Alziz A. A. and Hanafi A. S., "Experimental and numerical investigation of natural convection heat transfer in horizontal elliptic annuli", Journal of Applied Sciences Research, 4(2), pp. 138-155, 2008.

[14]. Xu Xu , Gonggang S. , Zitao Y. Yacai H. Liwu F. and Kefa C. ;"Numerical investigation of laminar natural convective heat transfer from a horizontal triangular cylinder to its concentric cylindrical enclosure"; International Journal of Heat and Mass Transfer 52 (2009) 3176–3186.

[15]. Yasin V. , Hakan F. O., Ahmet K., and Filiz O.; " Natural convection and fluid flow in inclined enclosure with a corner heater", Applied Thermal Engineering 29 (2009), pp.340–350

[16]. Mahfouz F. M., and Badr H. M., " Heat convection between two confocal elliptic tubes placed at different orientations", Advances in Applied Mathematics and Mechanics, Vol. 1, No. 5, pp. 639-663, October 2009.

[17]. Salam H. H. and Ahmed K. H., " Numerical investigation of natural convection phenomena in a uniformly heated circular cylinder immersed in square enclosure filled with air at different vertical locations", International Communications in Heat and Mass Transfer 37 (2010) 1115–1126.

[18]. Salam H. H. and Ahmed K. H.," Numerical Analysis of Steady Natural Convection of Water in Inclined Square Enclosure with Internal Heat Generation"; 2010 International Conference on Mechanical and Electrical Technology (ICMET 2010).

[19]. Xu X. A., Zitao Y. B., Yacai H., Liwu F. , Kefa C.**;** " A numerical study of laminar natural convective heat transfer arounda horizontal cylinder inside a concentric air-filled triangular enclosure"; International Journal of Heat and Mass Transfer 53 (2010) 345–355.

[20]. Zi-Tao Y., Xu X., Ya-Cai H., Li-Wu F., Ke-Fa C.; "Unsteady natural convection heat transfer from a heated horizontal circular cylinder to its air-filled coaxial triangular enclosure"; International Journal of Heat and Mass Transfer 54 (2011) 1563–1571.

[21] Han W., Chuang S., Xin-Lin X., He-ping T.; "Numerical investigation of laminar natural convection in a circular enclosure with a rectangle cylinder", Authorized licensed use limited to: IEEE Xplore. Downloaded on August 13,2011 at 13:42:16 UTC from IEEE Xplore. Restrictions apply.

[22] Fluent Inc**.** Technical Manual, 1998.

[23] Patankar S. V. "Numerical Heat Transfer and Fluid Flow", Hemisphere Publishing Corporation: Washington, DC, 1980.

[24] Versteeg H. K and Malalasekera W., "An introduction to computational fluid dynamics. The Finite Volume Method." Longman Scientific and Technical: New York, 1995.

[25] Patankar S. V, Spalding D. B. ,"A calculation procedure for heat, mass and momentum transfer in three-dimensional parabolic flows", International Journal of Heat and Mass Transfer 1972; 15:1777–1787.

[26] Choudhury D, "Study of two benchmark heat transfer problem using FLUENT", ASME Heat Transfer Div. Publ. HTD, vol. 255, 21–30, 29th National Heat Transfer Conference, 8–11 August 1993, Atlanta, GA, U.S.A.

[27] Said, S. A. M., Habib, M. A., Badr, H. M and Anwar, S., "Numerical investigation of natural convection inside an inclined parallel-walled channel", Int. J. for numerical methods in fluids, 2005; 49:569–582.

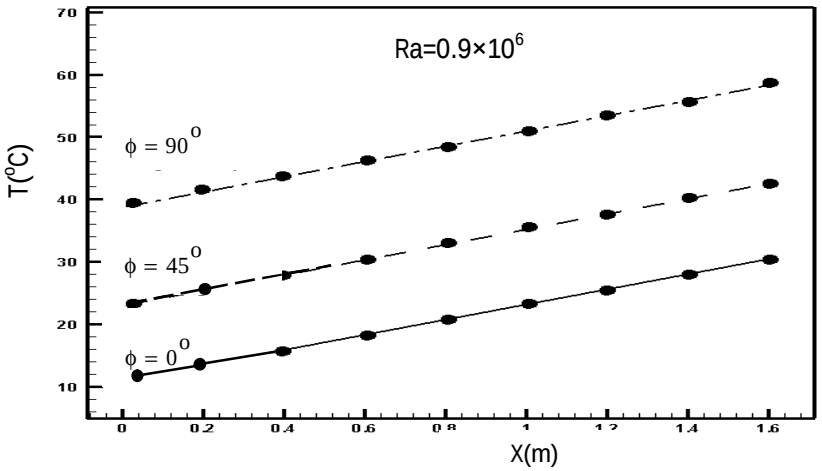

Figure.(3): Effect of angle of inclination on the temperature distribution along ellipticinner cylinder for Ra=0.6×10^6

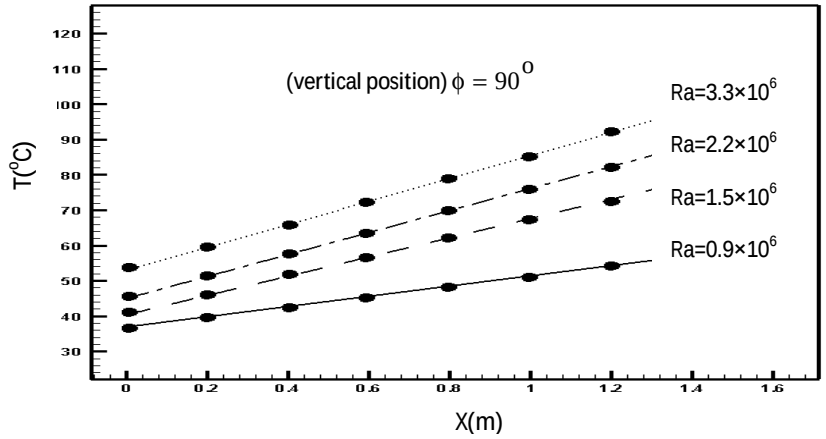

Figure.(4): Effect of Rayliegh number on the temperature distribution along elliptic inner cylinder for $f = 90^o$(vertical position).

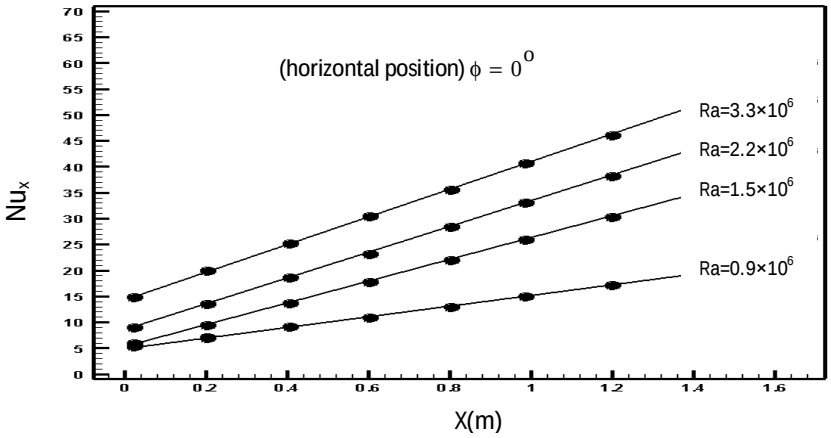

Figure.(5): Effect of Rayliegh number on the local Nusselt number along elliptic inner cylinder at $f = 0^o$(horizontal position).

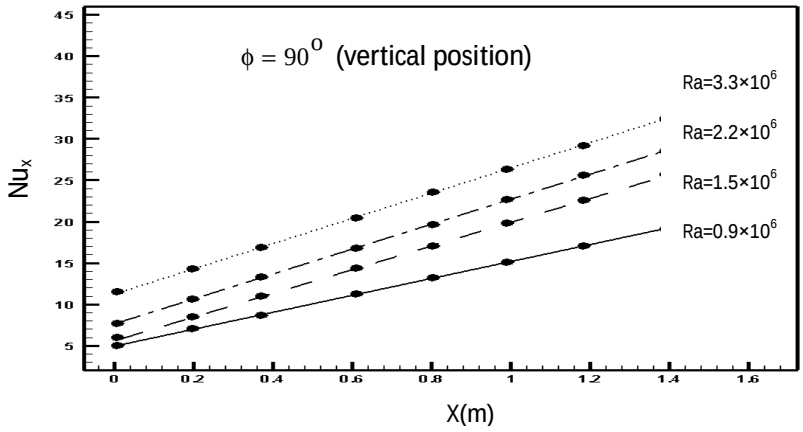

Figure.(6): Effect of Rayliegh number on the local Nusselt number along elliptic inner cylinder at $f = 90^o$(vertical position).

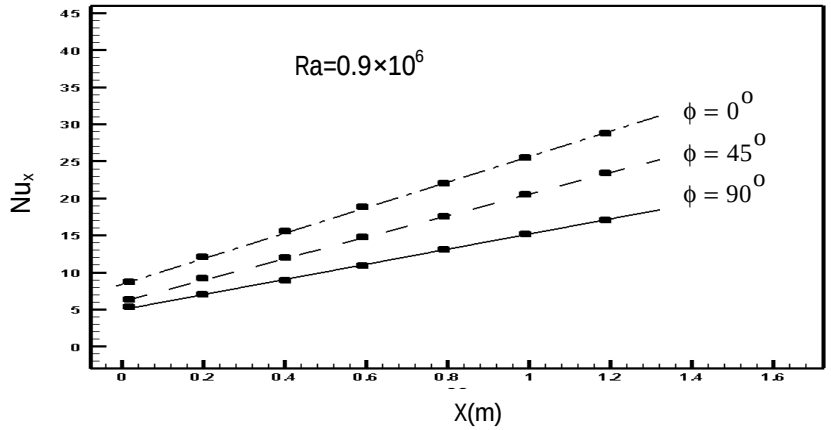

Figure.(7): Effect of angle of inclination on the local Nusselt number along elliptic inner cylinder for Ra=0.9×10^6.

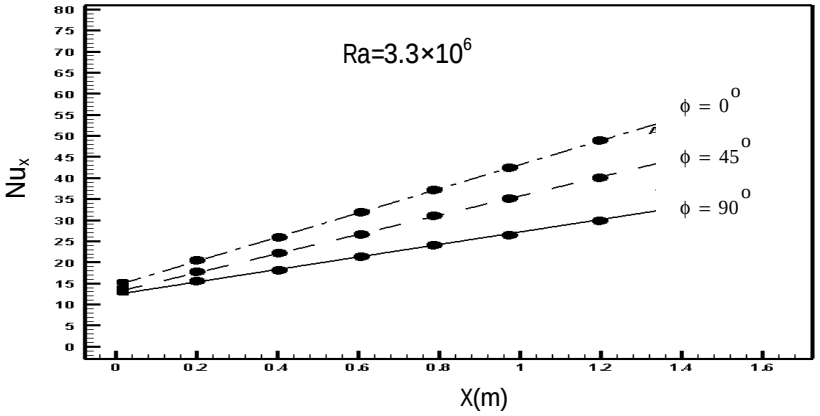

Figure.(8): Effect of angle of inclination on the local Nusselt number along elliptic inner cylinder for Ra=3.3×10^6.

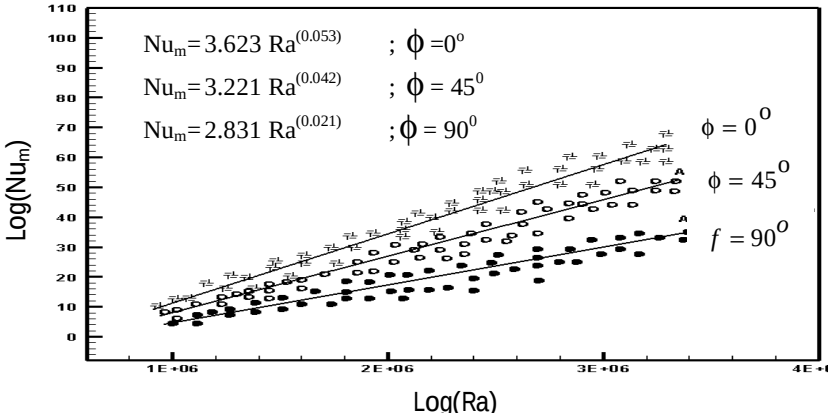

Figure.(9): Logarithm average Nusselt number versus logarithm Rayliegh number for three angles of inclination.

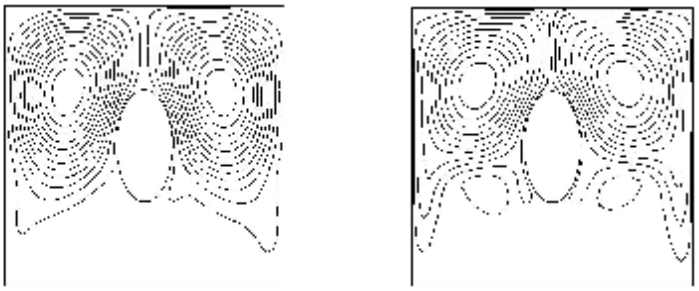

(a) HRR=3.93

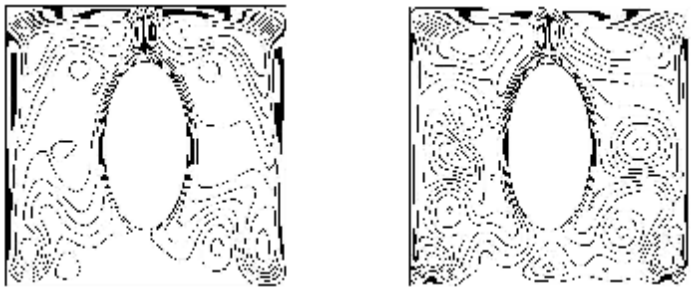

(b) HRR=2.62

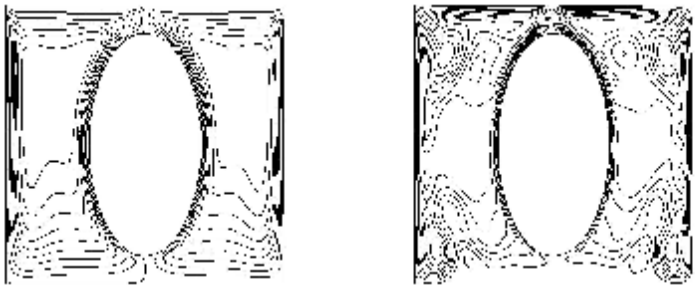

(c) HRR=1.97

Ra=0.9×10^6 Ra=3.3×10^6

Figure.(10): Stream lines for, $j = 0^o$.

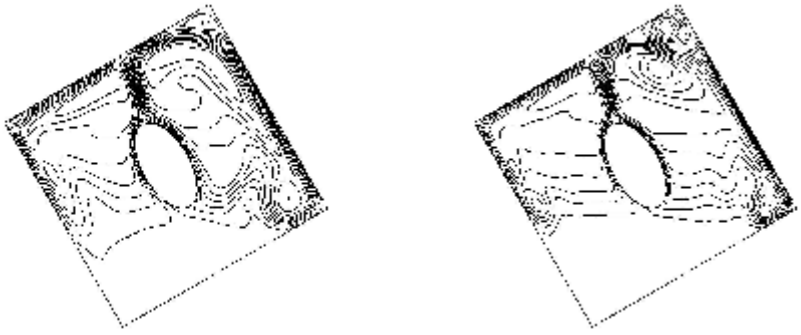

(a) HRR=3.93

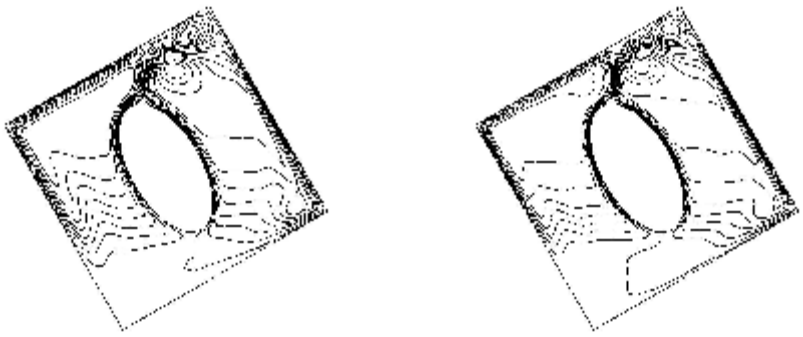

(b) HRR=2.62

(c) HRR=1.97

Ra=0.9×10^6 Ra=3.3×10^6

Figure.(11): Stream lines, $j = 30^o$.

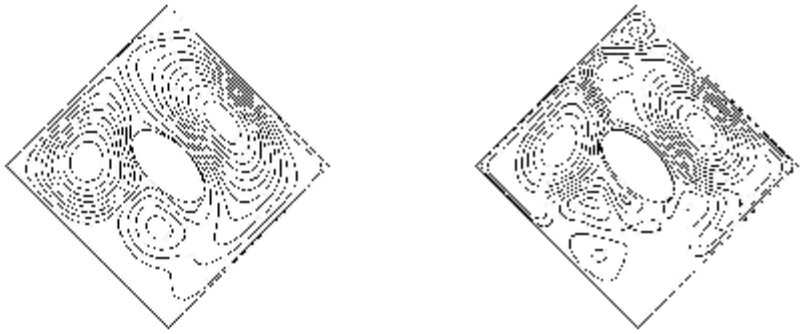

(a) HRR=3.93

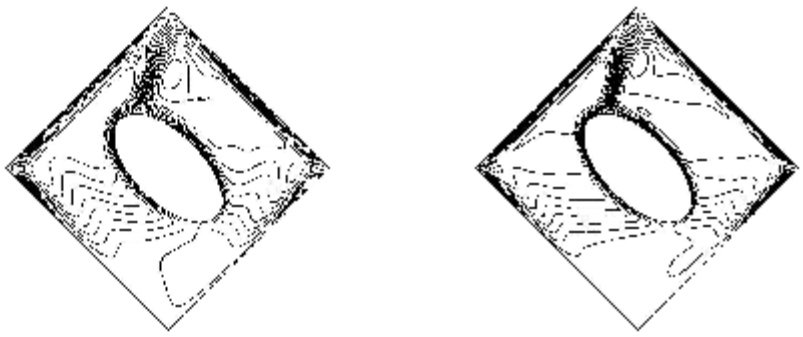

(b) HRR=2.62

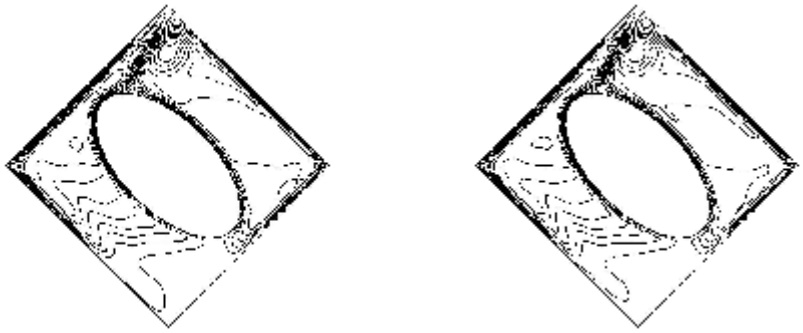

(c) HRR=1.97

Ra=0.9×10^6 Ra=3.3×10^6

Figure.(12): Stream lines, $j = 45^O$ **.**

(a) HRR=3.93

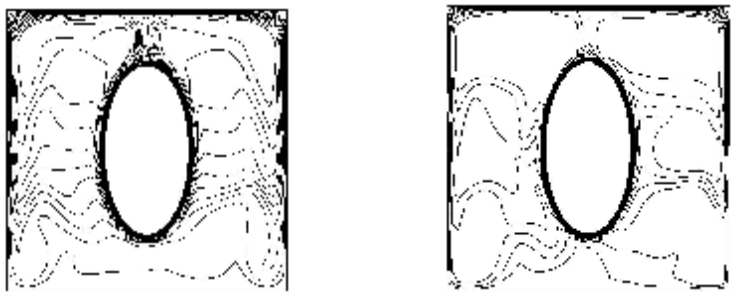

(b) HRR=2.62

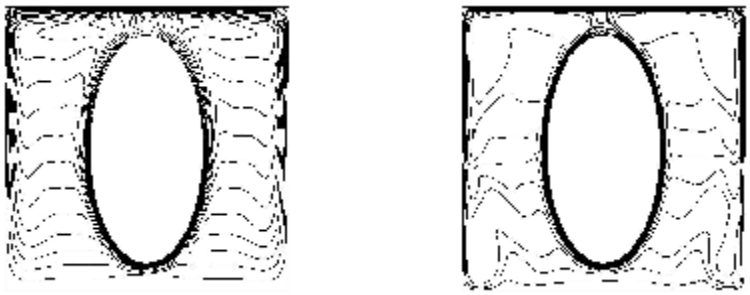

(c) HRR=1.97

Ra=0.9×10^6 Ra=3.3×10^6

Figure.(13): Temperature contours (isotherms), $\varphi = 0^o$.

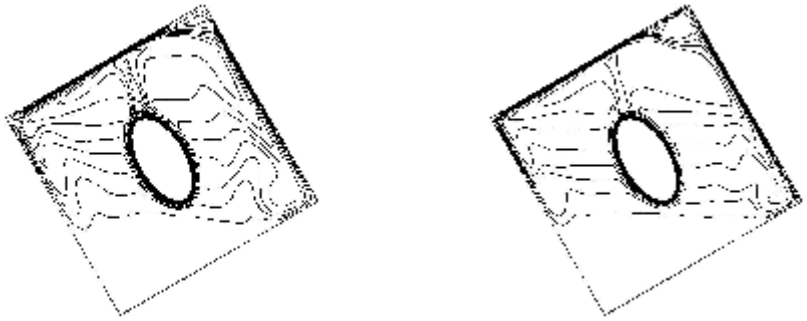

(a) HRR=3.93

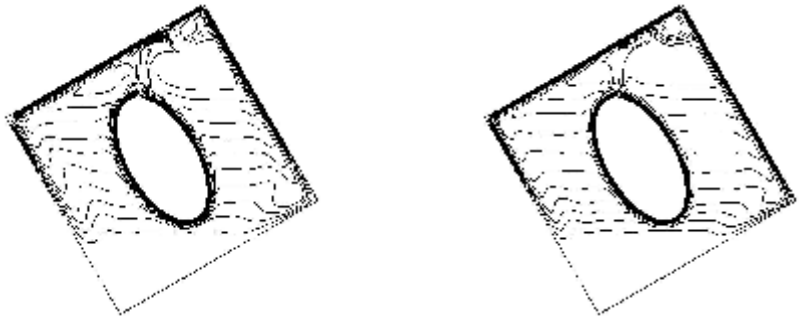

(b) HRR=2.62

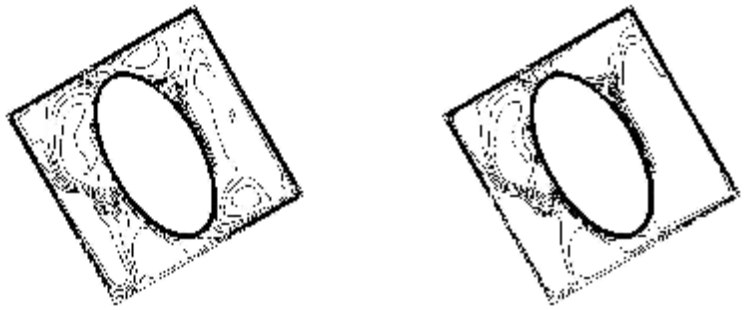

(c) HRR=1.97

Ra=0.9×10^6 Ra=3.3×10^6

Figure.(14): Temperature contours (isotherms), $j = 30^O$.

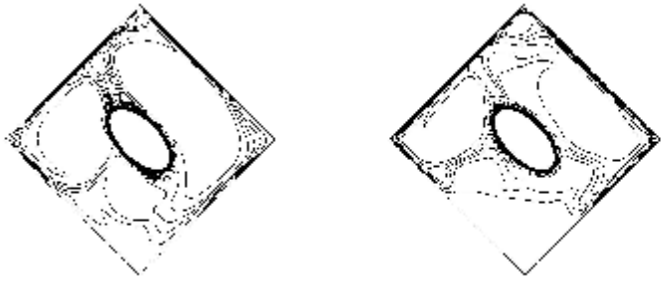

(a) HRR=3.93

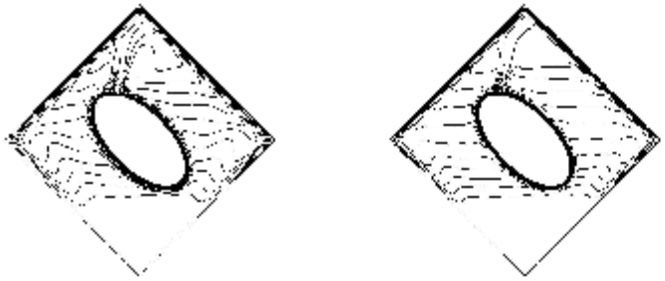

(b) HRR=2.62

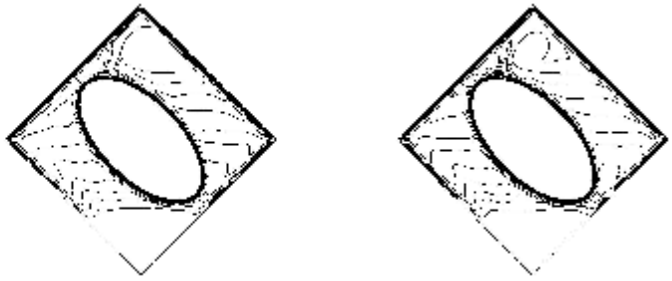

(c) HRR=1.97

Ra=0.9×10^6 Ra=3.3×10^6

Figure.(15): Temperature contours (isotherms), $j = 45^o$.

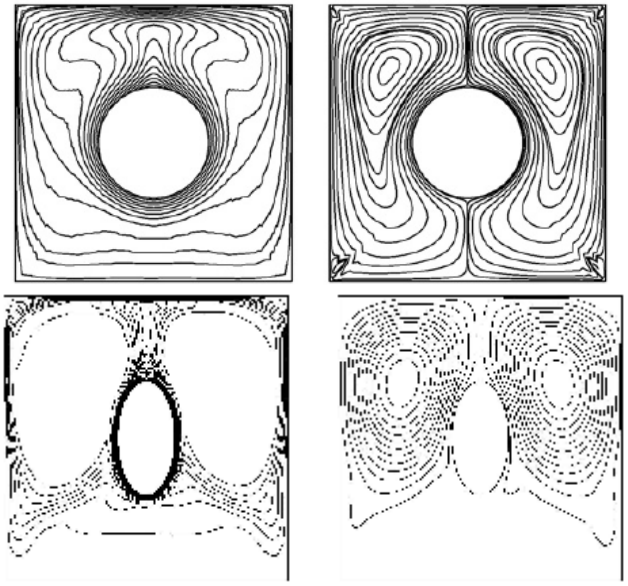

Figure.(16): Comparison of the temperature contours (left) and streamlines (right) between the present work ($Ra=0.9\times10^6$)and that of Salam and Ahmed ($Ra=10^6$)[18].

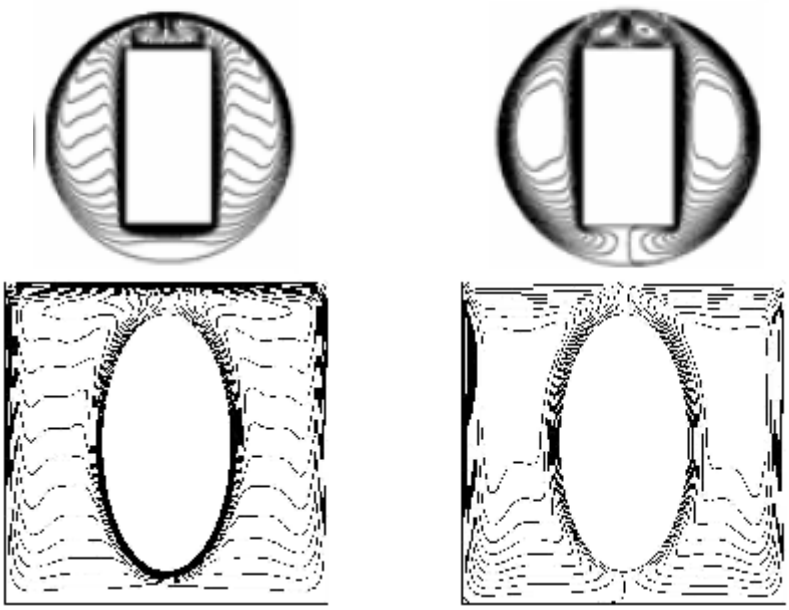

Figure.(17): Comparison of the temperature contours (left) and streamlines (right) between the present work ($Ra=0.9\times10^6$)and that of Hang Wang et al $Ra=10^6$ [21].